

DOI: 10.12401/j.nwg.2023116

赞比亚索卢韦齐地区新元古代石英二长岩的成因： 年代学、地球化学和 Sr–Nd–Hf 同位素约束

许康康^{1,2}, 孙凯^{1,2}, 吴兴源^{1,2}

(1. 中国地质调查局天津地质调查中心(华北地质科技创新中心), 天津 300170; 2. 中国地质调查局
南部非洲矿业研究所, 天津 300170)

摘要: 研究卢菲利安弧地区新元古代与裂谷作用有关的基性–中酸性岩浆作用, 对了解区域地壳生长和演化具有重要意义。研究表明, 卢菲利安弧地区发育有大量新元古代与裂谷作用有关的基性岩类, 但相关的中酸性岩岩浆作用却鲜有报道。笔者首次在赞比亚索卢韦齐地区发现有新元古代的石英二长岩体, 镍石 U–Pb 年龄为 (707.1 ± 3.0) Ma。地球化学特征显示该岩体具有较低的 MgO ($0.46\% \sim 0.76\%$)、CaO ($1.63\% \sim 1.76\%$)、K₂O ($0.49\% \sim 0.56\%$)、Mg[#] 值 ($8 \sim 13$) 和 Sr/Y 值 ($1.14 \sim 2.50$), 较高的 Al₂O₃ ($15.61\% \sim 16.02\%$)。岩体富集轻稀土和高场强元素 HFSEs (Nb, Ta, Hf), (La/Yb)_N 值为 $6.64 \sim 7.86$, 亏损 P, Ti, Zr 和大离子亲石元素 LILEs (Rb, Ba, Sr, K)。此外, 石英二长岩具有低的初始 $^{87}\text{Sr}/^{86}\text{Sr}$ 值 ($0.7058 \sim 0.7060$), 正的 $\varepsilon_{\text{Nd}}(t)$ 值 ($1.89 \sim 2.03$) 和镍石 $\varepsilon_{\text{Hf}}(t)$ 值 ($1.30 \sim 5.67$), 该特征与索卢韦齐地区新元古代早期辉长岩相似, 推测石英二长岩可能为新生的镁铁质下地壳在中–低压条件下部分熔融形成的。综合地质年代学和岩石成因研究, 笔者认为卢菲利安弧地区在新元古代经历了多阶段的地壳生长作用, 后期侵位的地幔岩浆加热早期就位于下地壳的镁铁质岩石并导致其部分熔融, 从而达到对地壳的改造作用。

关键词: 石英二长岩; 新元古代; 岩石成因; Lufilian 弧; 赞比亚

中图分类号: P581; P597

文献标志码: A

文章编号: 1009-6248(2023)05-0020-15

Petrogenesis of Neoproterozoic Quartz Monzonite in Solwezi Region, Zambia: Constraint from Geochronology, Geochemistry and Sr–Nd–Hf Isotopes

XU Kangkang^{1,2}, SUN Kai^{1,2}, WU Xingyuan^{1,2}

(1. China Geological Survey, Tianjin Centre (North China Center for Geoscience Innovation), Tianjin 300170, China; 2. Southern African
Mining Research Institute, China Geological Survey, Tianjin 300170, China)

Abstract: The study of mafic–intermediate and felsic magmatism related to Neoproterozoic rift in the Lufilian Arc is of great significance for understanding the crustal growth and secular evolution of the region. Studies have shown that there are a large number of Neoproterozoic mafic rocks which are related to rifting in the Lufilian arc, but a few of related intermediate and felsic magmatism are discovered. A Neoproterozoic quartz monzonite with a zircon U–Pb age of 707.1 ± 3.0 Ma was first discovered and reported in the Lufilian Arc. The plu-

收稿日期: 2023-04-03; 修回日期: 2023-06-11; 责任编辑: 姜寒冰

基金项目: 中国地质调查局项目(DD20190439、DD20551801), 国家重点研发计划课题“环太平洋和非洲成矿域战略性矿产信息及成矿规律”(2021YFC2901804)联合资助。

作者简介: 许康康(1986–), 男, 高级工程师, 主要从事地质矿产勘查与研究工作。E-mail: xukang06@163.com。

ton is characterized by relatively low MgO (0.46%~0.76%), CaO (1.63%~1.76%), K₂O (0.49%~0.56%), Mg[#] values (8~13) and Sr/Y ratios (1.14~2.50), as well as high Al₂O₃ content (15.61%~16.02%). REE-normalized patterns show enrichment in LREE with (La/Yb)_N of 6.64~7.86 and their primitive mantle-normalized trace element patterns are characterized by depletion of LILEs (Rb, Ba, Sr, K) and P, Ti, Zr and enrichment of HFSEs (Nb, Ta, Hf). They have a low initial ⁸⁷Sr/⁸⁶Sr ratios (0.7058~0.7060) with positive $\varepsilon_{\text{Nd}}(t)$ values (1.89~2.03) and their zircon $\varepsilon_{\text{Hf}}(t)$ values range from 1.30 to 5.67, their isotopic data are similar to those of the Neoproterozoic mafic intrusions in the Solwezi region, suggesting that the quartz monzonite were generated by partial melting of newly emplaced mafic lower crust. In combination with the studies of geochronology and petrogenesis, it is concluded that the Lufilian Arc experienced a multi-stage crustal growth in the Neoproterozoic, the late intrusive mantle magma heated the mafic rocks emplaced in the lower crust at early stage, resulting in partial melting and reworking the early crust.

Keywords: quartz monzonite; Neoproterozoic; petrogenesis; Lufilian arc; Zambia

卢菲利安弧(Lufilian Arc)是世界上著名的沉积型铜钴成矿带(Key et al., 2001; Cailteux et al., 2005; Muchez et al., 2008; El Desouky et al., 2009; Hitzman et al., 2010; Eglinger et al., 2013),位于非洲中部地区,从赞比亚西北部经刚果(金)加丹加省一直延伸到赞比亚铜带省内,整体为向北凸起的构造带,延伸约为700 km,宽约为150 km(Key et al., 2001; Katongo et al., 2004; Master et al., 2005; Batumike et al., 2006; 许康康等, 2021a)。大地构造位置上,卢菲利安弧位于刚果克拉通与卡拉哈里克拉通之间,为冈瓦纳超大陆聚合形成的新元古代—古生代造山带(Hanson et al., 1993; Dirks et al., 1999; Kampunzu et al., 1999; Vinyu et al., 1999; Porada et al., 2000; Katongo et al., 2004)。根据地质单元类型、变质和变形特征,卢菲利安弧可分为加丹加前陆盆地、外部褶皱逆冲带、穹隆区、复向斜带和加丹加高原5个构造带(图1)(De Swardt et al., 1965; Unrug, 1983; Porada, 1989; Kampunzu et al., 2000)。

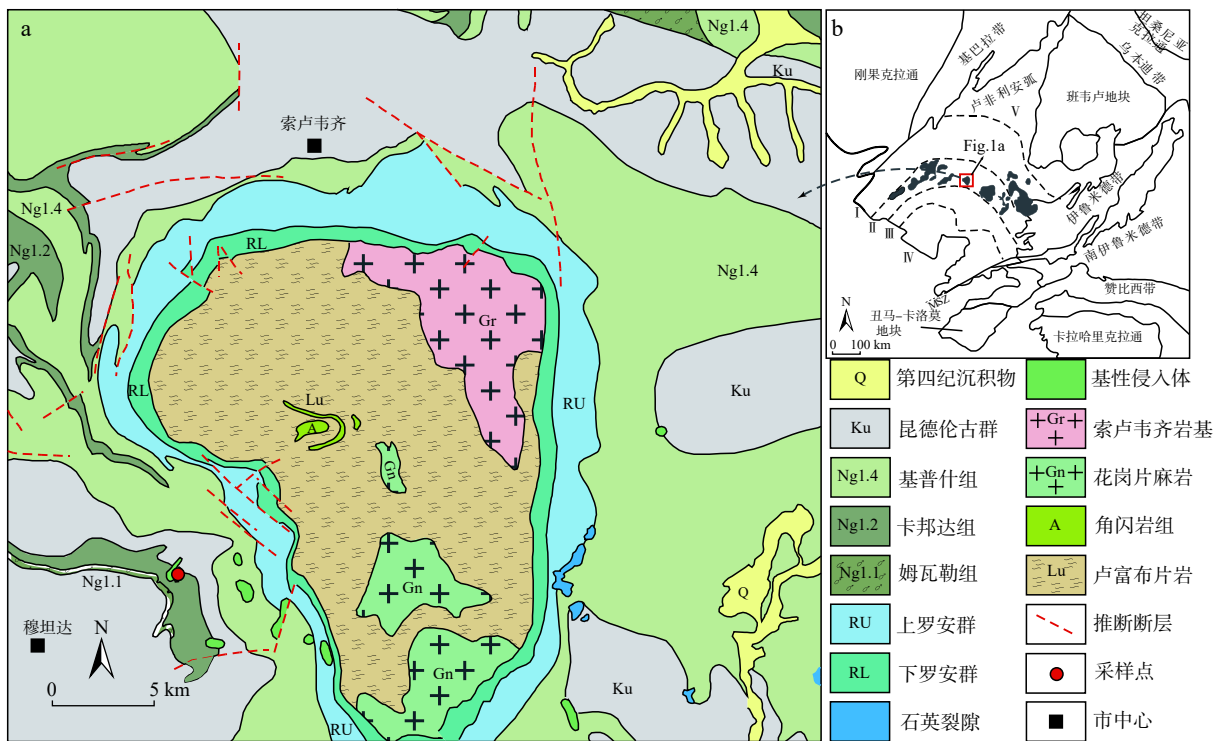
地幔活动是地壳演化的重要机制(Stein et al., 1994; Condie, 1998; Kemp et al., 2009),研究与地幔活动有关的基性-超基性岩以及中-酸性岩石的成因类型,对了解区域壳幔相互作用和地壳演化过程具有重要意义(Cai et al., 2015)。其中,二长岩类岩石在地球上分布广泛,通常来源于地壳深部演化的岩浆作用并包含有壳幔相互作用的重要信息(Smithies et al., 2000),为研究下地壳岩浆过程的重要“窗口”(Roberts et al., 2000; Zhao et al., 2010)。新元古代早期,卢菲利安弧地区为一套裂谷盆地系统(Hanson et al., 1993; Cailteux, 1994; Porada et al., 2000; Kampunzu et

al., 2000, 2009; Key et al., 2001; Barron et al., 2003),区域上广泛发育裂谷阶段地幔活动形成的基性岩体(Tembo et al., 1999; Kampunzu et al., 2000)。然而,相关的中-酸性岩石类型未见报道,从而造成对该地区裂谷作用时限和壳幔相互作用程度缺乏完整认识和充分证据,进而影响了对该地区地壳生长和改造过程的认知。笔者在赞比亚索卢韦齐地区首次报道有小规模的石英二长岩体出露,通过锆石U-Pb年代学、全岩地球化学和Sr–Nd–Hf同位素研究,初步探讨了其岩石成因、源区特征和地球动力学背景,从而为研究卢菲利安弧地区前寒武纪裂谷期间深部作用过程提供了一个重要的证据。

1 区域地质背景和岩石学特征

研究区位于赞比亚西北省穹窿区,穹隆区最主要特征为出现隐伏的基底岩石单元,并构成与卢菲利安弧造山运动期间形成的褶皱走向平行的弧形链(Kampunzu et al., 2000)。基底岩石主要为古元古代卢富布(Lufubu)群片岩、片麻岩,伊布尼(Eburnian)时期(约2200~1800 Ma)的花岗岩类(Key et al., 2001; Rainaud et al., 2005)以及不整合覆盖在卢富布群之上的古元古代—中元古代姆瓦(Muva)群石英岩和片岩(Rainaud et al., 2005)。新元古代的恩昌加花岗岩侵入到古元古代基底岩石内,其U-Pb锆石年龄为(883±10) Ma,代表了裂谷作用的开始(Katongo et al., 2004; Armstrong et al., 2005)。

卢菲利安弧内新元古代加丹加超群不整合覆盖在基底岩石之上,由约10 km厚的沉积岩和变质沉积



I. 外部褶皱逆冲带; II. 穹隆区; III. 复向斜带; IV. 加丹加高原; V. 前陆盆地

图1 赞比亚 Solwezi 地区石英二长岩分布(a)及南部非洲构造划分图(b)(据 Katongo et al., 2002; Johnson et al., 2005; Selley et al., 2005)

Fig. 1 (a) The distribution of quartz monzonite in Solwezi area and (b) the tectonic division of the Southern Africa

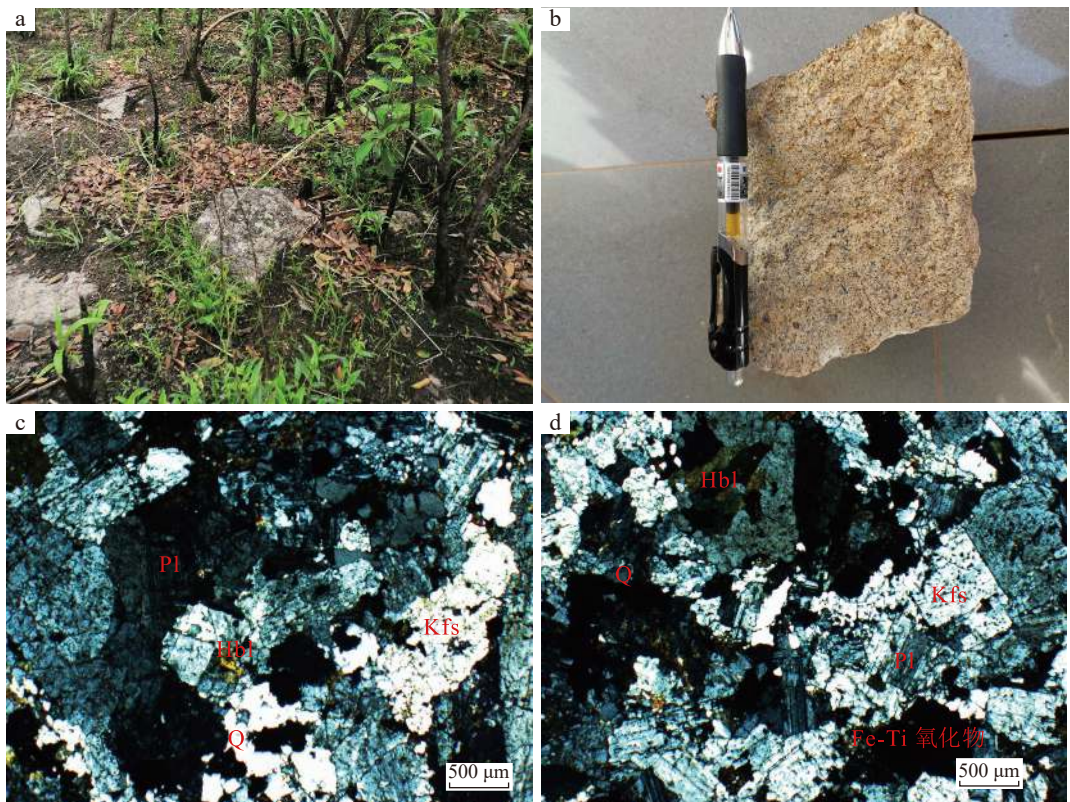
岩构成,从底到顶可以分为:罗安(Roan)群,恩古巴(Nguba)群、昆德伦古(Kundelungu)群和比亚诺(Biano)群(Cailteux et al., 1994, 2007, 2019; Batumike et al., 2007; 许康康等, 2021b)。罗安群底部为一套底砾岩,含有基底砾石和碎屑成分,后期逐渐过渡为碳酸盐岩、页岩互层和/或碳酸盐岩为主的沉积作用,最顶部的姆瓦夏(Mwashya)亚群以黑色页岩、白云质粉砂岩为主,反映了由浅水到深水的沉积环境变化(Cailteux et al., 2005)。该时期与裂谷作用演化有关的基性岩浆作用发育,如赞比亚西部姆瓦夏亚群内发育的基性火山岩U-Pb锆石年龄为(765±5)Ma(Kampunzu et al., 2000; Key et al., 2001)。恩古巴群和昆德伦古群具有相似的沉积序列,底部为一套陆源混杂岩(冰碛岩),上覆碳酸盐岩,顶部为硅质碎屑沉积岩(Batumike et al., 2006, 2007)。加丹加超群最晚期的比亚诺群岩性以长石砂岩、砾岩和页岩为主,发育近水平层理,代表了大陆碎屑磨拉石沉积作用类型(Cailteux et al., 2019)。昆德伦古群沉积作用阶段开始的卢菲利安造山作用导致区域岩石遭受绿片岩相-角闪岩相的变质作用,局部出现榴辉岩相(Porada et al., 2000; Rainaud et al., 2005; Naydenov et al., 2014)。

石英二长岩样品采集于索卢韦齐穹隆西部,距穆坦达市东北方向约12 km处的山坡上,测年样品(ZS05-3)的地理坐标为E 26°20'23", S 12°22'16"。该岩体规模较小,出露宽度约为15 m,具球形风化特征,由于覆盖严重,岩体与围岩的接触关系并不明确。根据赞比亚地质调查局1:10万地质图,该岩体侵入到恩古巴群地层内,周边发育有辉长岩体(图1b)。岩体新鲜面为灰白色-灰黄色,细粒结构,块状构造(图2a),主要由钾长石(35%)、斜长石(40%)、角闪石(12%)、石英(9%)和Ti-Fe氧化物等副矿物(4%)组成。钾长石呈半自形-他形,发育卡式双晶结构,表面多遭受轻微的高岭土化;斜长石呈长柱状,具典型的聚片双晶结构,表面发育轻微绢云母化。角闪石呈暗绿色,他形粒状,部分颗粒可见56°解理夹角。石英颗粒表面相对干净,多呈他形粒状充填在长石颗粒之间(图2b)。

2 分析方法

2.1 锆石 U-Pb 年代学

锆石分选在河北省廊坊市区域地质调查研究所完成,采用常规粉碎、浮选和电磁选方法进行分选,制



Pl. 斜长石; Hbl. 角闪石; Kfs. 钾长石; Q. 石英

图2 赞比亚穹窿区石英二长岩野外(a)、手标本(b)及显微照片(c、d)

Fig. 2 (a) Field photographs, (b) hand specimen and (c, d) micrographs of quartz monzonite in Dome area, Zambia

靶、阴极发光显微照相、透射光及反射光照射工作在北京锆年领航科技有限公司完成。锆石 U-Pb 同位素测年在天津地质调查中心实验室利用 LA-MC-ICP-MS 方法测定, 所用仪器为 Thermo Fisher 公司制造的 Neptune 多接收电感耦合等离子体质谱仪及与之配套的 New wave UP 193 nm 激光剥蚀系统。利用 193 nm FX 激光器对锆石进行剥蚀, 激光剥蚀的斑束直径为 35 μm。锆石年龄计算采用国际标准锆石 91500 作为外标, 元素含量采用人工合成硅酸盐玻璃 NIST SRM610 进行仪器最佳化, 每隔 8 个样品点测 2 次标样并进行 1 次仪器最佳化。数据处理采用 ICP MS Data Cal 程序 (Liu et al., 2008) 和 Isoplot 程序 (Ludwig, 2003) 进行加权平均年龄计算 (李艳广等, 2023)。

2.2 锆石 Lu-Hf 同位素

锆石 Lu-Hf 同位素测试在天津地质调查中心实验室完成, 采用配有 193 nm 的 LA-MC-ICP-MS 仪器上进行, 分析时采用 8~10 Hz 的激光频率、100 mJ 的激光强度和 50 μm 的激光束斑直径。激光剥蚀物质以 He 为载气送入 Neptune, 采用 GJ-1 作为监控标样,

具体测试过程见 Yuan 等 (2004)。为使 Hf 同位素分析与锆石 U-Pb 年龄分析相对应, 锆石 Hf 同位素的分析点与锆石 U-Pb 年龄分析点位于同一颗粒相同锆石晶域内, 可以认为所分析点的 Hf 同位素和 U-Pb 年龄是完全对应的。在计算 Hf 同位素的相关参数时, 采用的是同一颗粒锆石所测得的 U-Pb 年龄。在计算 ^{176}Lu 的衰变常数采用 $1.865 \times 10^{-11}/\text{a}$ (Scherer et al., 2001)。球粒陨石的 $^{176}\text{Lu} / ^{177}\text{Hf}$ 和 $^{176}\text{Hf} / ^{177}\text{Hf}$ 值分别为 0.033 2 和 0.282 772, 亏损地幔的 $^{176}\text{Lu} / ^{177}\text{Hf}$ 和 $^{176}\text{Hf} / ^{177}\text{Hf}$ 值分别为 0.038 4 和 0.283 25 (Griffin et al., 2000), 二阶段模式年龄分别采用平均地壳的 Lu/Hf 值为 -0.55, ($^{176}\text{Lu} / ^{177}\text{Hf}$)_{平均地壳} 为 0.015 (Griffin et al., 2002)。

2.3 全岩地球化学

岩石地球化学样品粉碎(200 目)在河北省廊坊市宇能岩矿公司加工完成。主量元素、稀土元素及微量元素测试分析均在天津地质调查中心实验室完成。主量元素采用 X 射线荧光光谱仪(XRF)测定, FeO 采用氢氟酸、硫酸溶样、重铬酸钾滴定容量法, 分析精度优于 2%。稀土元素和微量元素采用电感耦合等离

值特征(Belousova et al., 2002)。所有锆石点都位于谐和线上, $^{206}\text{Pb}/^{238}\text{U}$ 加权平均年龄为 $(707.1 \pm 3.0)\text{ Ma}$

(MSWD=0.26), 代表了石英二长岩的结晶年龄(图3b、图3c)。

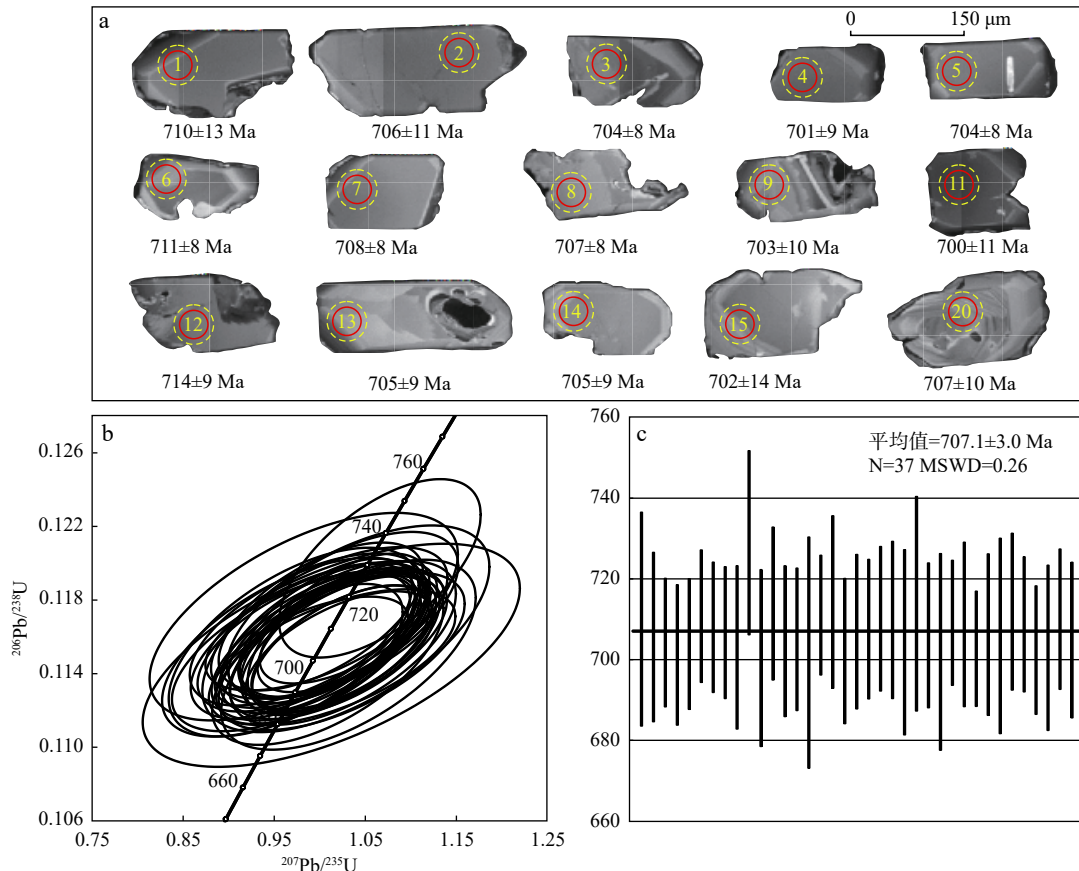


图3 石英二长岩代表性锆石CL图像(a)和锆石U-Pb年龄谐和图(b、c)

Fig. 3 (a) Cathodoluminescence (CL) images and (b, c) U-Pb concordia diagrams for representative zircons from quartz monzonite

3.2 岩石地球化学

石英二长岩主量元素含量分别为: SiO_2 (60.90%~61.71%)、 TiO_2 (0.97%~1.02%)、 CaO (1.63%~1.76%)、 Al_2O_3 (15.61%~16.02%) 和 FeO_t (8.16%~9.12%), 样品的 MgO 含量为 0.46%~0.76%, $\text{Mg}^{\#}$ 值为 8~13(表2)。在 $\text{Zr}/\text{TiO}_2-\text{Nb}/\text{Y}$ 图解上, 样品主要位于二长岩附近(图4a)。石英二长岩的 Na_2O 含量为 7.95%~8.62%, K_2O 含量为 0.49%~0.56%, $\text{Na}_2\text{O}/\text{K}_2\text{O}$ 值为 14.71~16.22, 位于碱性岩石系列范围内(图4b)。样品的 CaO 、 MgO 、 FeO_t 与 SiO_2 呈负相关(图5), TiO_2 、 P_2O_5 含量相对稳定, 反映了岩浆的分离结晶作用影响。

在原始地幔标准化图解上, 岩石富集高场强元素HFSEs(Nb 、 Ta 、 Hf), 亏损 P 、 Ti 、 Zr 和大离子亲石元素LILEs(Rb 、 Ba 、 Sr 、 K)(图6a)。此外, 岩石具有较高的Y含量(49.4×10^{-6} ~ 131×10^{-6})和低的Sr/Y值(1.14~2.50)。在球粒陨石标准化稀土元素配分模式图上, 岩

石具有一致的配分曲线, 稀土总量较高, ΣREE 值为 362.20×10^{-6} ~ 668.61×10^{-6} ; 轻稀土富集, 重稀土亏损, $(\text{La}/\text{Yb})_N$ 值为 6.64~7.86, $(\text{Gd}/\text{Yb})_N$ 值为 0.37~0.78, 并具有轻微 Eu 负异常($\delta\text{Eu}=0.86$ ~0.90)(图6b)。另外, 岩体具有轻微的 Ce 负异常, 可能与大洋裂谷时期的海水蚀变有关(Kampunzu et al., 2000)。

3.3 全岩 Sr-Nd 及锆石 Hf 同位素特征

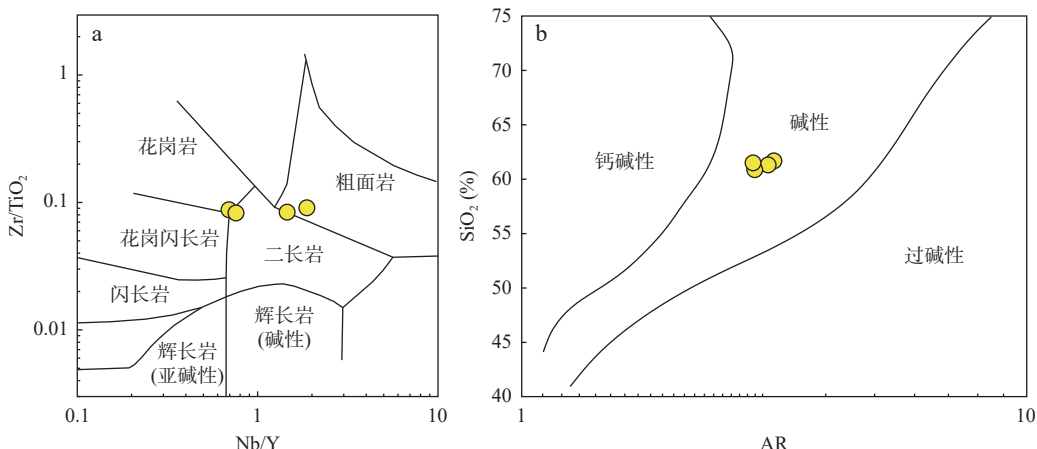
本次在锆石 U-Pb 定年同时, 挑选了 30 颗锆石进行原位 Lu-Hf 同位素分析, 分析点均位于已完成 U-Pb 年龄测试的锆石点上(但具有更大的范围)(图3a)。石英二长岩样品的锆石 $^{176}\text{Lu}/^{177}\text{Hf}$ 值多小于 0.002(表3), 显示锆石形成以后具有较低的放射性成因 Hf 积累, 有效的保留了初始的 $^{176}\text{Hf}/^{177}\text{Hf}$ 值(Patchett et al., 1982)。

计算初始 $\varepsilon_{\text{hf}}(t)$ 以及模式年龄时采用石英闪长岩结晶年龄 $t=707\text{ Ma}$ 进行校正, 结果表明 30 个测试点

表2 石英二长岩的主量元素(%)和微量元素(10^{-6})分析结果表Tab. 2 Major element (%) and trace element compositions (10^{-6}) for quartz monzonite

样品号	SiO ₂	Al ₂ O ₃	Fe ₂ O ₃	FeO	CaO	MgO	K ₂ O	Na ₂ O	TiO ₂	P ₂ O ₅	MnO	灼失	Cu	Pb	Zn	Cr	Ni	Co	Rb
ZS05-1	60.90	15.80	6.99	2.83	1.76	0.76	0.54	8.00	1.01	0.2	0.023	0.87	11.7	1.74	26.5	4.67	11.1	10.7	3.16
ZS05-2	61.71	16.02	7.67	1.26	1.65	0.46	0.55	8.62	1.02	0.24	0.015	0.64	11.1	1.53	26.2	0.61	8.43	9.34	2.35
ZS05-3	61.34	15.61	8.48	1.30	1.67	0.46	0.56	8.24	1.02	0.24	0.016	0.93	11.9	1.15	22.4	0.60	8.16	8.46	1.96
ZS05-4	61.53	15.83	6.86	2.70	1.63	0.74	0.49	7.95	0.97	0.14	0.03	0.82	10.8	1.33	26.3	2.76	11.9	10.2	1.57
样品号	Cs	Sr	Ba	V	Sc	Nb	Ta	Zr	Hf	Ga	U	Th	La	Ce	Pr	Nd	Sm	Eu	Gd
ZS05-1	0.04	154	66.2	6.96	26.1	89.9	5.31	848	31.3	34.3	1.70	8.69	78	147	26.3	105	20.9	6.01	19.1
ZS05-2	0.03	168	56.7	7.40	27.9	90.9	5.55	894	33.7	36.5	1.8	11.80	142	124	46.2	194	38.5	10.70	36.6
ZS05-3	0.03	134	49.0	5.22	25.4	89.5	5.28	844	32.0	33.0	1.46	8.39	128	130	42.4	180	36.2	10.00	34.1
ZS05-4	0.04	142	48.7	7.46	24.8	92.6	5.51	881	32.9	33.8	1.40	10.70	75	105	22.7	90	17.1	4.94	16.1
样品号	Tb	Dy	Ho	Er	Tm	Yb	Lu	Y	Mg [#]	Th/U	ΣREE	δEu	δCe	(La/Yb) _N	⁸⁷ Sr/ ⁸⁶ Sr(t)	ε _{Nd(t)}	T _{DM2} (Ma)		
ZS05-1	2.98	15.2	2.85	8.49	1.18	7.92	1.22	61.7	13	5.11	442.25	0.90	0.78	6.65	0.7058	1.89	1243		
ZS05-2	5.79	30.5	5.71	16.20	2.23	14.1	2.08	131.0	9	6.56	668.61	0.86	0.37	6.79	/	/	/		
ZS05-3	5.50	28.2	5.22	15.00	2.02	13.0	1.90	118.0	8	5.75	631.54	0.86	0.42	6.64	0.7060	2.03	1232		
ZS05-4	2.38	11.8	2.19	6.74	0.95	6.39	1.01	49.4	13	7.64	362.20	0.90	0.61	7.86	/	/	/		

注: Mg[#]=100×(MgO/40.32)/(MgO/40.32+FeO/71.94)。

图4 石英二长岩Zr/TiO₂-Nb/Y图解(a)(据 Middlemost, 1994)和AR-SiO₂图解(b)(据 Wright, 1969)Fig. 4 (a) Zr/TiO₂-Nb/Y and (b) AR-SiO₂ diagrams for quartz monzonite

的 $^{176}\text{Hf}/^{177}\text{Hf}$ 值为0.282 383~0.282 504, Hf同位素初始比值 $\epsilon_{\text{Hf}}(t)$ 为1.30~5.67, 平均值为3.48, T_{DM2} 值为1 265~1 540 Ma。在 $\epsilon_{\text{Hf}}(t)$ -t图解上, 所有测点位于亏损地幔和球粒陨石演化线之间(图7a)。

石英二长岩Sr-Nd同位素变化均较小(表2), 同位素比值通过锆石U-Pb年龄($t=707$ Ma)进行校正后, 其初始的 $^{87}\text{Sr}/^{86}\text{Sr}$ 值为0.705 8~0.706 0, $\epsilon_{\text{Nd}}(t)$ 值为1.89~2.03(图7b), 对应的二阶段亏损模式年龄为1 232~1 243 Ma。

4 讨论

4.1 蚀变作用影响及分离结晶过程

石英二长岩样品的烧失量(LOI)为0.64%~0.92%, 暗示样品可能经历了一定程度的后期蚀变作用。然而, 高场强元素Th、Ti、Nb、Ta、Zr、Hf、Y和REEs等元素在蚀变和风化作用过程中通常保持相对稳定(Barnes et al., 1985; Wang et al., 2013)。Zr通常被用来

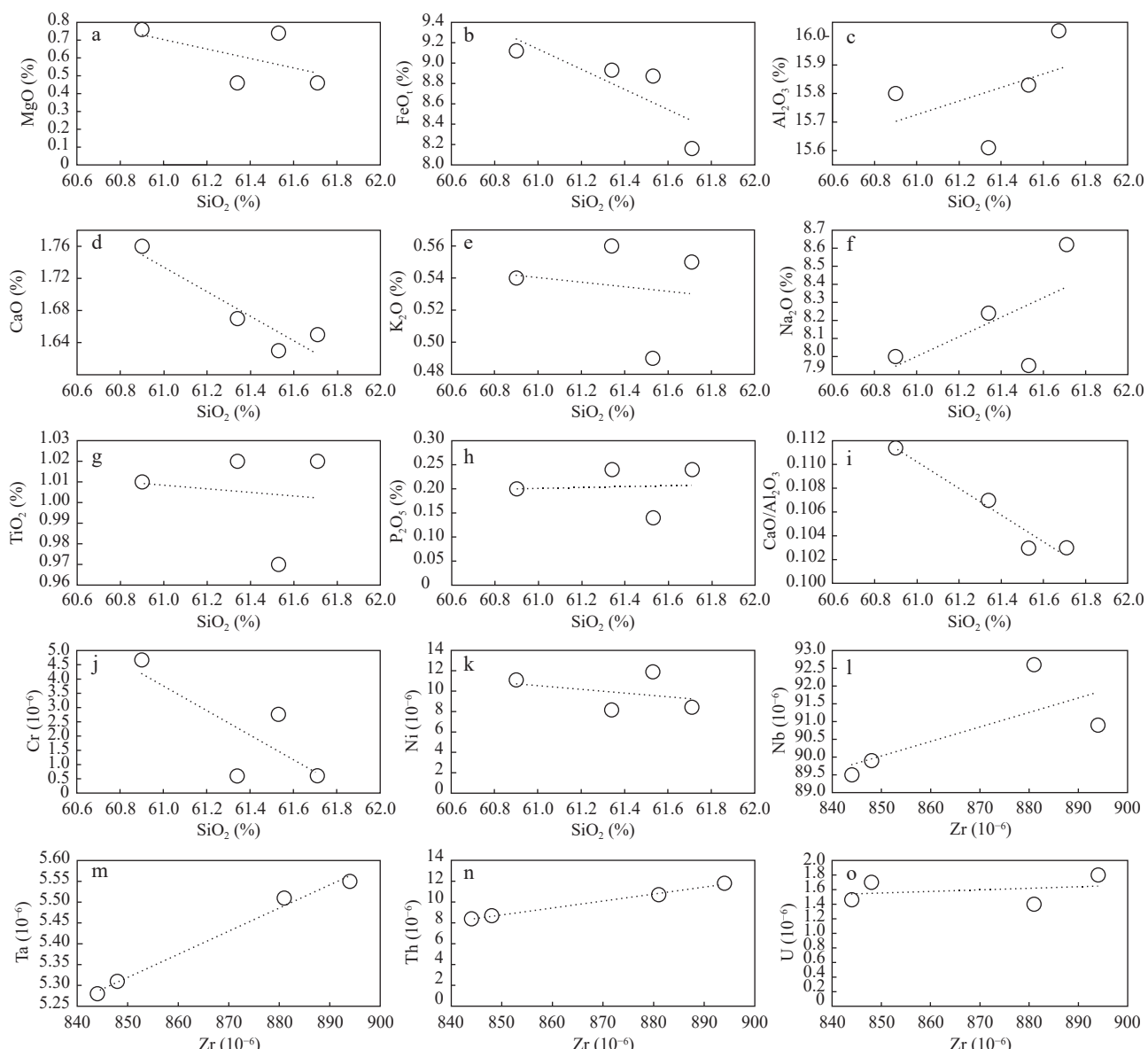


图5 石英二长岩主量元素和代表性微量元素Harker图解
Fig. 5 Harker plots of major and selected trace elements for quartz monzonite

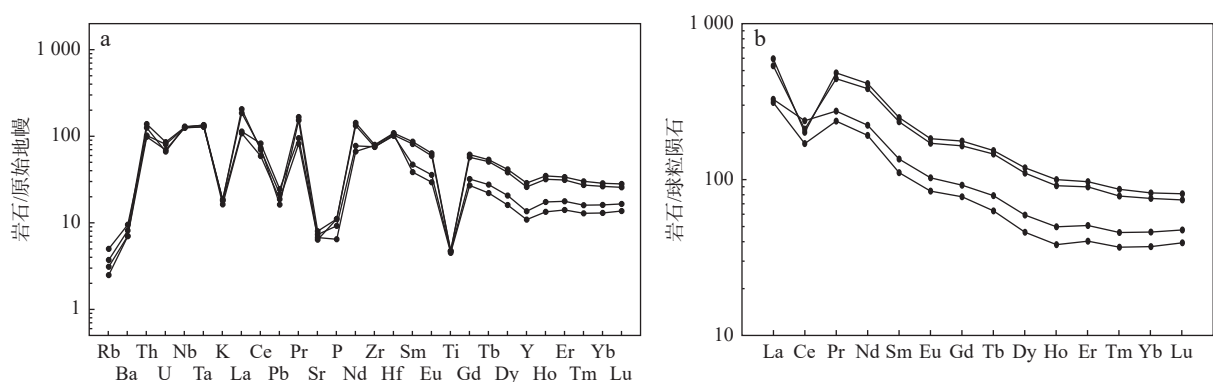


图6 原始地幔标准化微量元素(a)和球粒陨石标准化稀土元素(b)图解(据Sun et al., 1989)
Fig. 6 (a) Primitive Mantle (PM) normalized trace elements and (b) Chondrite-normalized REE elements diagrams of quartz monzonite

表3 石英二长岩锆石原位Lu-Hf同位素结果表

Tab. 3 Zircon in situ Lu-Hf isotope data of quartz monzonite

点号	年龄(Ma)	$^{176}\text{Yb}/^{177}\text{Hf}$	2σ	$^{176}\text{Lu}/^{177}\text{Hf}$	2σ	$^{176}\text{Hf}/^{177}\text{Hf}$	2σ	$\varepsilon_{\text{Hf}}(t)$	2σ	T_{DM1}	2σ	T_{DM2}	2σ
01	707	0.0361	0.0008	0.0012	0.0000	0.282383	0.000022	1.30	0.95	1233	30	1540	50
02	707	0.0331	0.0005	0.0011	0.0000	0.282462	0.000023	4.15	0.92	1118	32	1360	52
03	707	0.0491	0.0006	0.0015	0.0000	0.282466	0.000027	4.07	1.02	1127	38	1366	61
04	707	0.0384	0.0005	0.0012	0.0000	0.282497	0.000024	5.34	0.94	1072	34	1286	55
05	707	0.0314	0.0005	0.0010	0.0000	0.282495	0.000022	5.34	0.84	1071	30	1286	49
06	707	0.0382	0.0005	0.0013	0.0000	0.282471	0.000020	4.35	0.80	1113	29	1348	47
07	707	0.0345	0.0005	0.0011	0.0000	0.282425	0.000021	2.80	0.82	1173	30	1446	48
08	707	0.0387	0.0002	0.0012	0.0000	0.282421	0.000024	2.62	0.93	1181	34	1457	55
09	707	0.0440	0.0007	0.0014	0.0000	0.282400	0.000024	1.82	0.95	1215	34	1507	54
10	707	0.0542	0.0013	0.0017	0.0000	0.282426	0.000025	2.57	1.01	1189	36	1460	57
11	707	0.0315	0.0001	0.0010	0.0000	0.282393	0.000022	1.69	0.92	1215	31	1515	51
12	707	0.0287	0.0002	0.0010	0.0000	0.282401	0.000020	2.05	0.81	1200	28	1493	46
13	707	0.0245	0.0003	0.0008	0.0000	0.282490	0.000024	5.23	0.95	1073	34	1293	55
14	707	0.0347	0.0001	0.0012	0.0000	0.282415	0.000027	2.43	1.02	1188	38	1469	60
15	707	0.0322	0.0005	0.0011	0.0000	0.282477	0.000026	4.64	1.10	1100	36	1330	60
16	707	0.0480	0.0003	0.0016	0.0000	0.282473	0.000023	4.29	0.89	1118	33	1352	53
17	707	0.0296	0.0006	0.0010	0.0000	0.282390	0.000023	1.63	0.91	1217	33	1519	53
18	707	0.0349	0.0002	0.0012	0.0000	0.282435	0.000024	3.13	0.97	1160	34	1425	55
19	707	0.0418	0.0003	0.0014	0.0000	0.282488	0.000025	4.91	0.95	1092	35	1313	56
20	707	0.0226	0.0001	0.0008	0.0000	0.282417	0.000023	2.67	0.91	1174	32	1454	53
21	707	0.0348	0.0007	0.0011	0.0000	0.282395	0.000024	1.72	0.92	1216	33	1513	54
22	707	0.0369	0.0009	0.0012	0.0000	0.282470	0.000026	4.35	0.99	1112	37	1348	59
23	707	0.0671	0.0007	0.0022	0.0000	0.282452	0.000026	3.25	1.00	1169	37	1417	59
24	707	0.0281	0.0003	0.0009	0.0000	0.282483	0.000025	4.95	1.01	1086	35	1310	57
25	707	0.0314	0.0006	0.0011	0.0000	0.282452	0.000022	3.78	0.98	1133	32	1384	53
26	707	0.0333	0.0006	0.0011	0.0000	0.282411	0.000026	2.33	0.98	1191	36	1475	58
27	707	0.0293	0.0021	0.0010	0.0001	0.282504	0.000024	5.67	0.97	1057	34	1265	56
28	707	0.0432	0.0001	0.0015	0.0000	0.282436	0.000023	3.05	0.96	1167	32	1430	52
29	707	0.0272	0.0001	0.0010	0.0000	0.282432	0.000025	3.14	0.95	1157	35	1424	57
30	707	0.0359	0.0007	0.0012	0.0000	0.282488	0.000021	5.02	0.87	1085	30	1306	49

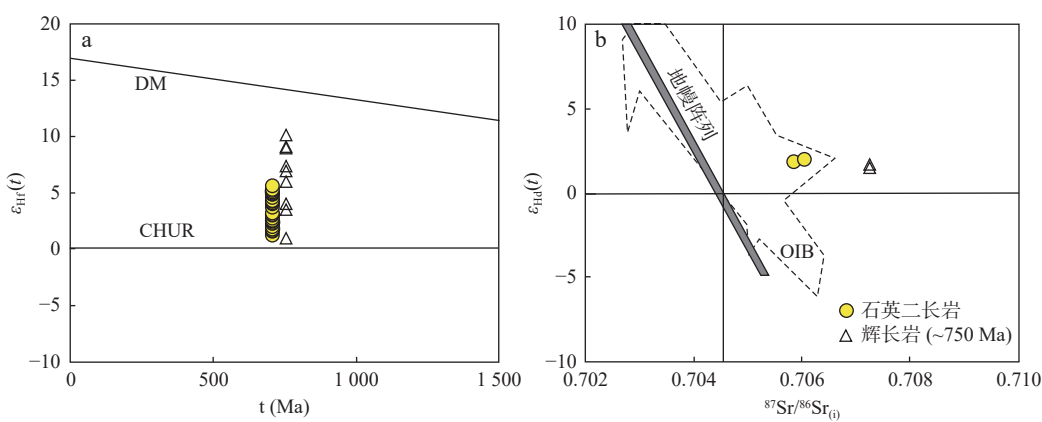


图7 石英二长岩锆石 $\varepsilon_{\text{Hf}}(t)$ - $^{207}\text{Pb}/^{206}\text{Pb}$ 年龄图解(a)和 $\varepsilon_{\text{Nd}}(t)$ - $^{87}\text{Sr}/^{86}\text{Sr}_{\text{(i)}}$ 图解(b)
Fig. 7 (a) $\varepsilon_{\text{Hf}}(t)$ -zircon $^{207}\text{Pb}/^{206}\text{Pb}$ age and (b) $\varepsilon_{\text{Nd}}(t)$ - $^{87}\text{Sr}/^{86}\text{Sr}$ for quartz monzonite

检测其他不相容元素的活动性(Rolland et al., 2009)。在双变量图解中, Nb、Ta、Th、U与Zr具有明显的正相关性(图5l~图5o),且样品具有近平行的稀土和多元素图解(图6),暗示这些元素在变质和蚀变作用过程中受影响程度较低,可以代表原始组分(Cai et al., 2015)。

石英二长岩显示一定的分离结晶趋势,在Harker图解中,随着SiO₂含量的增加,CaO、MgO、FeO、Cr、Ni含量降低而全碱含量升高(图5a),表明岩浆可能经历了橄榄石、辉石、角闪石和Ti-Fe氧化物的分离结晶作用。此外,CaO/Al₂O₃值与SiO₂呈负相关性,表明富钙矿物相(单斜辉石)为可能的分离结晶矿物(图5i)。P₂O₅含量随SiO₂变化相对稳定,表明磷灰石未发生明显的分离结晶作用(图5h)。在微量元素蛛网图上,Sr具亏损特征,在稀土元素标准化图解上,Eu具有轻微负异常($\delta\text{Eu}=0.86\sim0.90$),表明斜长石发生分离结晶作用。

4.2 岩石成因

大陆地壳整体为安山质组分,具有镁铁质下地壳向以花岗质为主上地壳的垂直演化分带特征,中性-酸质岩浆岩的成因研究是认识大陆地壳演化的关键(Annen et al., 2006; Cawood et al., 2013; Condie et al., 2013; Zhou et al., 2015)。石英二长岩的SiO₂含量为60.90%~61.71%,小于65%,为中性岩浆。关于中性岩浆岩的成因,目前主要有以下3种模式:①受俯冲板块流体和熔体改造的地幔楔内方辉橄榄岩的部分熔融作用(Tatsumi, 1982; Carmichael, 2002; Parmanet et al., 2004)。②浅部地壳岩浆房内或位于/靠近莫霍面的深部地壳内地幔来源岩浆的分离结晶作用(Kushiro, 1969; Arth et al., 1972; Shaw et al., 1993)。③下地壳镁铁质岩石的脱水部分熔融作用(Watters, 1978; Jung et al., 2002; Flierdt et al., 2003; 任云伟等, 2022),同时混染或未混染有硅酸质岩浆(Cantagrel et al., 1984; Clemens et al., 1987; Gao et al., 2004; Annen et al., 2006)。

地幔楔来源或地幔分离结晶作用来源的中性岩通常具有较高的MgO含量和Mg[#]值,从而与富Mg的橄榄岩相达到平衡(Tatsumi, 1982; Grove et al., 2003),而低Mg[#]值的闪长岩则不能与地幔岩石达到平衡(Annen et al., 2006)。石英二长岩具有较低的Cr($0.60\times10^{-6}\sim4.67\times10^{-6}$)、Ni($8.16\times10^{-6}\sim11.90\times10^{-6}$)和Mg[#]值(8~13),与地幔来源的高镁闪长岩明显不符(Stern et

al., 1991; Zhao et al., 2010),排除了地幔楔部分熔融或地幔岩浆分离结晶作用的可能性。研究表明,地幔来源的母岩浆在分离结晶约80%的基性矿物后,Th含量可以升高至 3.0×10^{-6} (Rapp et al., 1995),石英二长岩具有高的Th含量($8.39\times10^{-6}\sim11.80\times10^{-6}$),明显高于 3.0×10^{-6} ,暗示其不为地幔岩浆高程度分离结晶的产物。

石英二长岩具有较低的MgO和Mg[#]值,与来自加厚下地壳的埃达克质岩石或1.0~4.0 Gpa压力条件下角闪岩和榴辉岩实验熔体相似(图8a),暗示岩浆可能来源于下地壳的部分熔融。较高的Th含量和Th/U值,同样位于下地壳熔体区域(图8b)。研究认为新就位的下地壳镁铁质侵入体部分熔融可以产生大量的硅质岩浆,尤其是在高热流区域(Beard et al., 1991; Roberts et al., 1993; Rapp et al., 1995),其初始的同位素值与镁铁质源区相似(Zhao et al., 2010)。赞比亚索卢韦齐地区发育有大面积的辉长岩体(~750 Ma)(Tembo et al., 1999; Kampunzu et al., 2000; Barron et al., 2003),岩体的全岩 $\varepsilon_{\text{Nd}}(t)$ 值(1.53~1.76)、锆石 $\varepsilon_{\text{Hf}}(t)$ 值(0.97~10.14)与石英二长岩的全岩 $\varepsilon_{\text{Nd}}(t)$ 值(1.89~2.03)、锆石 $\varepsilon_{\text{Hf}}(t)$ 值(1.30~5.67)相近(图7)。石英二长岩位于高铝玄武质实验熔体区域且具有与低K橄榄质拉斑玄武岩和低K太古宙绿岩相似的K₂O含量,与碱性玄武质实验熔体相比,岩石具有低的MgO、CaO和高的FeO、Na₂O含量(图9),暗示石英二长岩的原岩可能为富Al、低K的钙碱性玄武质岩石,该化学性质也与区域上新元古代辉长岩体相当(Tembo et al., 1999; Kampunzu et al., 2000),进一步表明石英二长岩可能为新就位的镁铁质下地壳部分熔融的产物。

研究认为,Al₂O₃的含量可以用来评估压力条件(Rapp et al., 1995)。当P<1.6 Gpa时,实验熔体具有小于15%的Al₂O₃含量,角闪石、斜长石和斜方辉石为残留相;当P>1.6 Gpa时,实验熔体的Al₂O₃含量大于15%且残留组分包括角闪石、斜长石、单斜辉石和石榴子石;当P=2.0~3.0 Gpa时,实验熔体与不含斜长石但富含石榴子石的角闪岩、榴辉岩或麻粒岩达到平衡(Cai et al., 2015)。部分熔融实验同样表明高压条件下生成的熔体具有高的Sr含量和Sr/Y值,低的Y和HREEs含量(Petford et al., 1996)。石英二长岩的Al₂O₃含量为15.61%~16.02%,Sr/Y值较低(1.14~2.87),表明熔融作用可能发生在1.6 Gpa左右的中-低

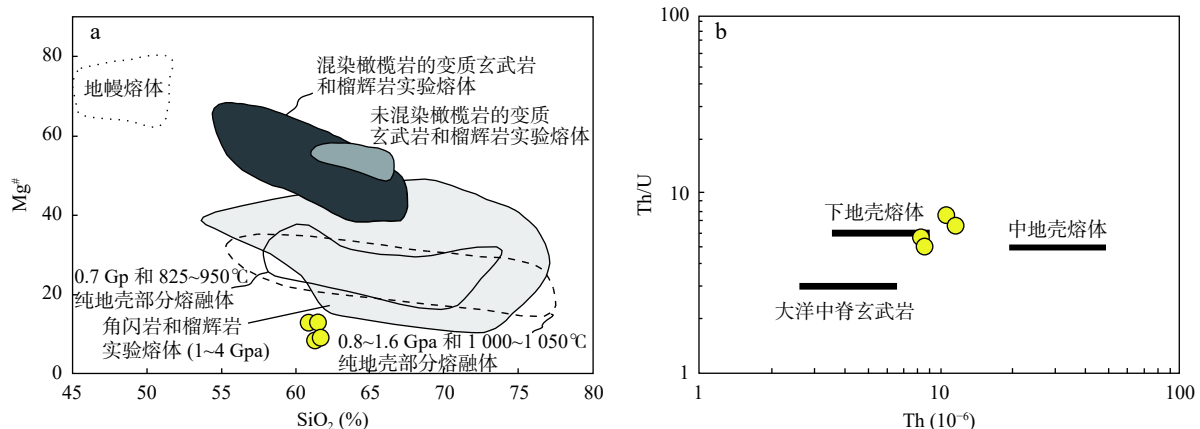


图8 石英二长岩的 $Mg^{\#}$ - SiO_2 图解(a)(据 Wang et al., 2005)和 Th/U-Th 图解(b)(据 Rudnick et al., 2003)

Fig. 8 (a) $Mg^{\#}$ - SiO_2 and (b) Th/U-Th diagrams for quartz monzonite

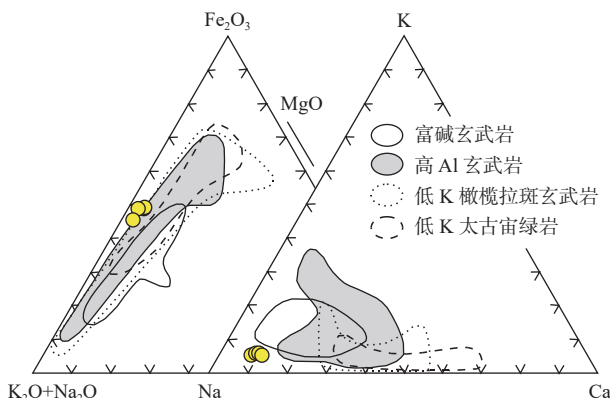


图9 石英二长岩 AFM 图解和摩尔 Na-K-Ca 图解(据 Zhao et al., 2010)

Fig. 9 Ternary AFM and molar Na-K-Ca diagrams for quartz monzonite

压条件下。石英二长岩的 MgO 含量为 0.46%~0.76%， TiO_2 含量为 0.97%~1.02%，位于 Rapp 等(1995)的实

验熔体区域，表明镁铁质下地壳的熔融温度为 1 000~1 100 °C(图 10)。实验研究表明玄武质岩石脱水熔融程度为 5%~10% 时可以产生酸性岩浆，而熔融程度达 20%~40% 时，则产生高 Al_2O_3 的酸性-中性岩浆(Rapp et al., 1995)。石英二长岩具有低的 SiO_2 含量(60.90%~61.71%)和较高的 Al_2O_3 含量，暗示石英二长岩可能为镁铁质下地壳熔融程度为 20%~40% 的产物。

总之，赞比亚索卢韦齐地区石英二长岩可能为大陆地壳内镁铁质岩石在中-低压(~ 1.6 Gpa)、高温(1 000~1 100 °C)条件下脱水熔融的产物，其原岩可能为裂谷作用早阶段侵位于下地壳的幔源岩浆组分。

4.3 地球动力学意义

研究表明地幔柱活动是地壳形成的重要机制(Stein et al., 1994; Condie, 1998; Kemp et al., 2009)，卢菲利安弧地区在新元古代早期处于裂谷作用环境

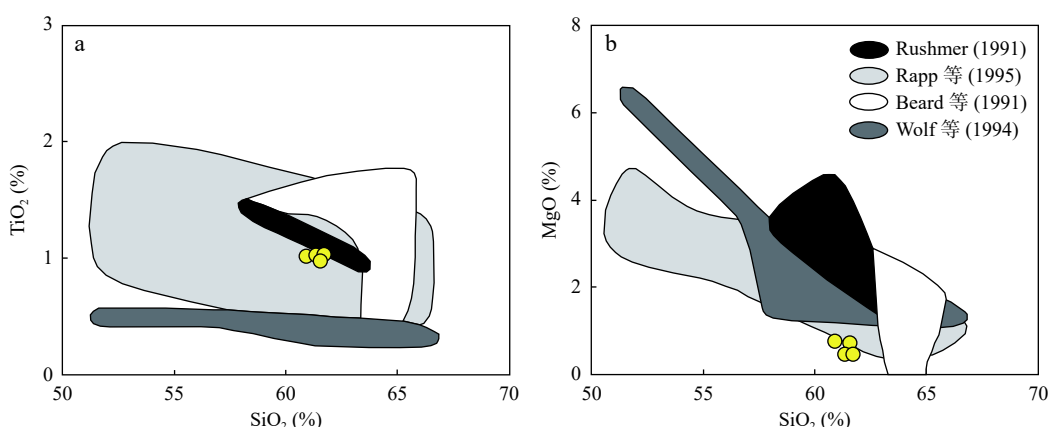


图10 石英二长岩的 SiO_2 - TiO_2 (a)和 SiO_2 - MgO (b)图解(据 Jung et al., 2002)

Fig. 10 (a) SiO_2 - TiO_2 and (b) SiO_2 - MgO diagrams for quartz monzonite

(Kampunzu et al., 2000; Master et al., 2005), 与全球 Rodinia 超大陆裂解时期一致(陆松年, 1998; 徐焱等, 2020)。该时期卢菲利安弧内发育大规模的基性岩浆作用, 为地幔部分熔融的产物(Tembo et al., 1999; Kampunzu et al., 2000), 年龄主要为 765~745 Ma, 如西北省卢瓦乌(Lwawu)地区基性火山岩的锆石 U-Pb 年龄为(765±5)Ma(Kepp et al., 2001), 索卢韦齐地区辉长岩的年龄为(745±7.8)Ma 和(753±8.6) Ma(Barron et al., 2003)。在基特韦地区新发现有晚期的辉长岩体, 锆石 U-Pb 年龄为(702.9±3.2)Ma, 表明卢菲利安弧地区至少经历了两期的地壳生长作用。

研究认为新生镁铁质地壳的熔融作用是大陆地壳分异的一种重要机制(Zhao et al., 2010; Cai et al., 2015), 下地壳镁铁质岩石在高温条件下的脱水熔融需要大量热量, 而热量的来源通常与地幔玄武质岩浆底侵作用有关(Clemens, 1990; Vielzeuf et al., 1990)。赞比亚索卢韦齐地区石英二长岩的锆石 U-Pb 年龄为(707.1±3.0)Ma, 岩石成因研究表明其为早期侵位的镁铁质下地壳(~750 Ma)部分熔融的产物, 且年龄与晚期的辉长岩体(~703 Ma)相近, 推测后期高温地幔玄武质岩浆在侵位形成新地壳的同时加热早期形成的下地壳岩石, 导致脱水熔融形成石英二长岩岩浆, 从而导致卢菲利安弧地区地壳发生分异改造作用。

5 结论

(1) 石英二长岩的锆石 U-Pb 年龄为(707.1±3.0) Ma, 为新元古代裂谷作用时期岩浆作用。

(2) 石英二长岩的 MgO、CaO、K₂O 含量较低, Al₂O₃ 含量较高, Mg[#]值和 Sr/Y 值较低, 富集 LREEs 和 HFSE(Nb、Ta、Hf), 亏损 LILEs(Rb、Ba、Sr、K) 和 P、Ti、Zr, 全岩 ε_{Nd}(t) 值和锆石 ε_{Hf}(t) 值与区域上 ~750 Ma 的辉长岩体相当。岩石地球化学特征表明, 石英二长岩可能为早期镁铁质下地壳在中-低压、高温条件下部分熔融的产物。

(3) 卢菲利安弧地区在裂谷作用时期至少经历了两期的地壳生长作用, 且后期侵位的地幔玄武质岩浆加热早期就位的下地壳岩石导致部分熔融, 从而达到对前期地壳的分异改造作用。

参考文献(References):

李艳广, 靳梦琪, 汪双双, 等. LA-ICP-MS U-Pb 定年技术相关

- 问题探讨[J]. 西北地质, 2023, 56(4): 274~282.
- LI Yanguang, JIN Mengqi, WANG Shuangshuang, et al. Exploration of Issues Related to the LA-ICP-MS U-Pb Dating Technique[J]. Northwestern Geology, 2023, 56(4): 274~282.
- 陆松年. 新元古时期 Rodinia 超大陆研究进展述评[J]. 地质评论, 1998, 44(5): 489~495.
- LU Songnian. A Review of Advance in the Research on the Neoproterozoic Rodinia Supercontinent[J]. Geological Review, 1998, 44(5): 489~495.
- 任云伟, 张家辉, 田辉, 等. 天镇-怀安地区新太古代末二长花岗岩的成因及动力背景[J]. 华北地质, 2022, 45(2): 76~86.
- REN Yunwei, ZHANG Jiahui, TIAN Hui, et al. Petrogenesis and geodynamic settings of monzonitic granite at the end of the Neoarchean in Tianzhen-Huai'an area[J]. North China Geology, 2022, 45(2): 76~86.
- 徐焱, 张世红. 塔里木克拉通在 Rodinia 中的位置——研究进展与问题[J]. 地质调查与研究, 2020, 43(2): 169~176.
- XU Yan, ZHANG Shihong. The position of Tarim Craton in Rodinia: advances and problems[J]. Geological Survey and Research, 2020, 43(2): 169~176.
- 许康康, 孙凯, 何胜飞, 等. 非洲中部新元古代 Lufilian 弧地区地质特征、成矿时代及构造演化历史[J]. 地质与勘探, 2021a, 57(03): 676~692.
- XU Kangkang, SUN Kai, HE Shengfei, et al. Geological Characteristics and Metallogenic Age and Tectonic Evolution History of Neoproterozoic Lufilian Arc in Central Africa[J]. Geology and Prospecting, 2021a, 57(03): 676~692.
- 许康康, 孙凯, 何胜飞, 等. 赞比亚西北省 Solwezi 地区石榴云母片岩的碎屑锆石 U-Pb 年龄及其地质意义[J]. 华北地质, 2021b, 44(03): 1~3.
- XU Kangkang, SUN Kai, HE Shengfei, et al. Detrital zircon U-Pb dating of the garnet mica schist and its geological implications in the Solwezi area, Northwestern Zambia[J]. North China Geology, 2021b, 44(03): 1~3.
- Annen C, Blundy J D, Sparks R S J. The genesis of intermediate and silicic magmas in deep crustal hot zones[J]. Journal of Petrology, 2006, 47(3): 505~539.
- Armstrong R A, Master S, Robb L J. Geochronology of the Nchanga granite, and constraints on the maximum age of the Katanga Supergroup, Zambian Copperbelt[J]. Journal of African Earth Sciences, 2005, 42(1~5): 32~40.
- Arth J G, Hanson G N. Quartz diorites derived by partial melting of eclogite or amphibolite at mantle depths[J]. Contributions to Mineralogy and Petrology, 1972, 37(2): 161~174.
- Barnes S J, Naldrett A J, Gorton M P. The origin of the fractionation of platinum-group elements in terrestrial magmas[J]. Chemical Geology, 1985, 53: 303~323.
- Barron J W. Stratigraphy, metamorphism, and tectonic history of the

- Solwezi area, Northwest Province, Zambia: Integrating geological field observations and airborne geophysics in the interpretation of regional geology[D]. Colorado School of Mines, Golden, CO., USA, 2003: 1–233.
- Batumike M J, Kampunzu A B, Cailteux J H. Petrology and geochemistry of the Neoproterozoic Nguba and Kundelungu Groups, Katangan Supergroup, southeast Congo: Implications for provenance, paleoweathering and geotectonic setting[J]. *Journal of African Earth Sciences*, 2006, 44(1): 97–115.
- Batumike M J, Cailteux J L H, Kampunzu A B. Lithostratigraphy, basin development, base metal deposits, and regional correlations of the Neoproterozoic Nguba and Kundelungu rock successions, central African Copperbelt[J]. *Gondwana Research*, 2007, 11(3): 432–447.
- Beard J S, Lofgren G E. Dehydration melting and water-saturated melting of basaltic and andesitic greenstones and amphibolites at 1, 3, and 6. 9 kb[J]. *Journal of Petrology*, 1991, 32(2): 365–401.
- Belousova E, Griffin W L, O'Reilly S Y, et al. Igneous zircon: trace element composition as an indicator of source rock type[J]. *Contributions to Mineralogy and Petrology*, 2002, 143: 602–622.
- Cai Y, Wang Y, Cawood P A, et al. Neoproterozoic crustal growth of the Southern Yangtze Block: Geochemical and zircon U-Pb geochronological and Lu-Hf isotopic evidence of Neoproterozoic diorite from the Ailaoshan zone[J]. *Precambrian Research*, 2015, 266: 137–149.
- Cailteux J. Lithostratigraphy of the Neoproterozoic Shaba-type (Zaire) Roan Supergroup and metallogenesis of associated stratiform mineralization[J]. *Journal of African Earth Sciences*, 1994, 19(4): 279–301.
- Cailteux J L H, Kampunzu A B, Lerouge C, et al. Genesis of sediment-hosted stratiform copper–cobalt deposits, central African Copperbelt[J]. *Journal of African Earth Sciences*, 2005, 42(1–5): 134–158.
- Cailteux J L H, Kampunzu A B, Lerouge C. The Neoproterozoic Mwashya–Kansuki sedimentary rock succession in the Central African Copperbelt, its Cu–Co mineralisation, and regional correlations[J]. *Gondwana Research*, 2007, 11(3): 414–431.
- Cailteux J, Putter T D. The Neoproterozoic Katanga Supergroup (D. R. Congo): State-of-the-art and revisions of the lithostratigraphy, sedimentary basin and geodynamic evolution[J]. *Journal of African Earth Sciences*, 2019, 150: 522–531.
- Cantagrel J M, Didier J, Gourgaud A. Magma mixing: origin of intermediate rocks and “enclaves” from volcanism to plutonism[J]. *Physics of the earth and planetary interiors*, 1984, 35(1–3): 63–76.
- Carmichael I S. The andesite aqueduct: perspectives on the evolution of intermediate magmatism in west-central (105–99 W) Mexico[J]. *Contributions to Mineralogy and Petrology*, 2002, 143(6): 641–663.
- Cawood P A, Hawkesworth C J, Dhuime B. The continental record and the generation of continental crust[J]. *Bulletin*, 2013, 125(1–2): 14–32.
- Clemens A. The granulite–granite connection[J]. In: Vielzeuf D, Vidal P, eds. *Granulites and Crustal Evolution*[M]. Dordrecht, Kluwer, 1990: 25–36.
- Clemens J D, Vielzeuf D. Constraints on melting and magma production in the crust[J]. *Earth and Planetary Science Letters*, 1987, 86(2–4): 287–306.
- Condie K C. Episodic continental growth and supercontinents: a mantle avalanche connection[J]. *Earth and Planetary Science Letters*, 1998, 163(1–4): 97–108.
- Condie K C, Kröner A. The building blocks of continental crust: evidence for a major change in the tectonic setting of continental growth at the end of the Archean[J]. *Gondwana Research*, 2013, 23(2): 394–402.
- De Swardt A M J, Gerrard P, Simpson J. Major zones of transcurrent dislocation and superposition of orogenic belts in part of Central Africa[J]. *Geological Society of America BulletinBull*, 1965, 76(1): .89–1.
- Dirks P H G M, Sithole T A. Eclogites in the Makuti gneisses of Zimbabwe: implications for the tectonic evolution of the Zambezi Belt in southern Africa[J]. *Journal of Metamorphic Geology*, 1999, 17(6): 593–612.
- Eglinger A, André-Mayer A S, Vanderhaeghe O. Geochemical signatures of uranium oxides in the Lufilian belt: from unconformity-related to syn-metamorphic uranium deposits during the Pan-African orogenic cycle[J]. *Ore Geology Reviews*, 2013, 54: 197–213.
- El Desouky H A, Muchez P, Cailteux J. Two Cu–Co sulfide phases and contrasting fluid systems in the Katanga Copperbelt, Democratic Republic of Congo[J]. *Ore Geology Reviews*, 2009, 36(4): 315–332.
- Flierdt T V D, Hoernes S, Jung S, et al. Lower crustal melting and the role of open-system processes in the genesis of syn-orogenic quartz diorite–granite–leucogranite associations: constraints from Sr–Nd–O isotopes from the Bandombaa Complex, Namibia[J]. *Lithos*, 2003, 67: 205–226.
- Gao S, Rudnick R L, Yuan H, et al. Recycling lower continental crust in the North China craton[J]. *Nature*, 2004, 432(7019): 892–897.
- Griffin W L, Pearson N J, Belousova E, et al. The Hf isotope composition of cratonic mantle: LAM-MC-ICPMS analysis of zircon megacrysts in kimberlites[J]. *Geochimica et Cosmochimica Acta*, 2000, 64(1): 133–147.

- Griffin W L, Wang X, Jackson S E, et al. Zircon chemistry and magma mixing, SE China: In-situ analysis of Hf isotopes, Tonglu and Pingtan igneous complexes[J]. *Lithos*, 2002, 61(3-4): 237-269.
- Grove T L, Elkins-Tanton L T, Parman S W, et al. Fractional crystallization and mantle-melting controls on calc-alkaline differentiation trends[J]. *Contributions to Mineralogy and Petrology*, 2003, 145(5): 515-533.
- Hanson R E, Wardlaw M S, Wilson T J, et al. U-Pb zircon ages from the Hook granite massif and Mwembeshi dislocation: Constraints on pan-African deformation, plutonism, and transcurrent shearing in central Zambia[J]. *Precambrian Research*, 1993, 63: 189-209.
- Hitzman M W, Selley D, Bull S. Formation of sedimentary rock-hosted stratiform copper deposits through Earth history[J]. *Economic Geology*, 2010, 105(3): 627-639.
- Johnson S P, Rivers T, De Waele B. A review of the Mesoproterozoic to early Palaeozoic magmatic and tectonothermal history of south-central Africa: implications for Rodinia and Gondwana[J]. *Journal of the Geological Society*, 2005, 162(3): 433-450.
- Jung S, Hoernes S, Mezger K. Synorogenic melting of mafic lower crust: constraints from geochronology, petrology and Sr, Nd, Pb and O isotope geochemistry of quartz diorites (Damara orogen, Namibia)[J]. *Contributions to Mineralogy and Petrology*, 2002, 143(5): 551-566.
- Kampunzu A B, Cailteux J. Tectonic evolution of the Lufilian Arc (Central Africa Copperbelt) during Neoproterozoic Pan African orogenesis[J]. *Gondwana Research*, 1999, 2(3): 401-421.
- Kampunzu A B, Tembo F, Matheis G, et al. Geochemistry and tectonic setting of mafic igneous units in the Neoproterozoic Katangan Basin, Central Africa: Implications for Rodinia breakup[J]. *Gondwana Research*, 2000, 3(2): 125-153.
- Kampunzu A B, Cailteux J L H, Kamona A F, et al. Sediment-hosted Zn-Pb-Cu deposits in the Central African Copperbelt[J]. *Ore Geology Reviews*, 2009, 35(3-4): 263-297.
- Katongo C, Koeberl C, Reimold W U, et al. Remote sensing, field studies, petrography, and geochemistry of rocks in central Zambia: no evidence of a meteoritic impact in the area of the Lukanga Swamp[J]. *Journal of African Earth Sciences*, 2002, 35(3): 365-384.
- Katongo C, Koller F, Kloetzli U, et al. Petrography, geochemistry, and geochronology of granitoid rocks in the Neoproterozoic-Paleozoic Lufilian-Zambezi belt, Zambia: Implications for tectonic setting and regional correlation[J]. *Journal of African Earth Sciences*, 2004, 40(5): 219-244.
- Kemp A I S, Hawkesworth C J, Collins W J, et al. Isotopic evidence for rapid continental growth in an extensional accretionary orogen: The Tasmanides, eastern Australia[J]. *Earth and Planetary Science Letters*, 2009, 284(3-4): 455-466.
- Key R M, Liyungu A K, Njamu F M, et al. The western arm of the Lufilian Arc in NW Zambia and its potential for copper mineralization[J]. *Journal of African Earth Sciences*, 2001, 33(3-4): 503-528.
- Kushiro I. The system forsterite-diopside-silica with and without water at high pressures[J]. *American Journal of Science*, 1969, 267(A): 269-294.
- Liu S, Hu R Z, Gao S, et al. U-Pb zircon age, geochemical and Sr-Nd-Pb-Hf isotopic constraints on age and origin of alkaline intrusions and associated mafic dikes from Sulu orogenic belt, Eastern China[J]. *Lithos*, 2008, 106: 365-379.
- Ludwig K R. User's Manual for Isoplot 3.00, a Geochronological Toolkit for Microsoft Excel[M]. Geochronological Center, Special Publication No. 4, Berkeley, 2003: 25-32.
- Master S, Rainaud C, Armstrong R A, et al. Provenance ages of the Neoproterozoic Katanga Supergroup (Central African Copperbelt), with implications for basin evolution[J]. *Journal of African Earth Sciences*, 2005, 42(1-5): 41-60.
- Middlemost E A K. Naming materials in the magma/igneous rock system[J]. *Earth Science Reviews*, 1994, 37: 215-224.
- Muchez P, Vanderhaeghen P, El Desouky H, et al. Anhydrite pseudomorphs and the origin of stratiform Cu-Co ores in the Katangan Copperbelt (Democratic Republic of Congo)[J]. *Mineralium Deposita*, 2008, 43(5): 575-589.
- Naydenov K V, Lehmann J, Saalmann K, et al. New constraints on the Pan-African Orogeny in Central Zambia: A structural and geochronological study of the Hook Batholith and the Mwembeshi Zone[J]. *Tectonophysics*, 2014, 637: 80-105.
- Parman S W, Grove T L. Harzburgite melting with and without H_2O : Experimental data and predictive modeling[J]. *Journal of Geophysical Research: Solid Earth*, 2004, 109(B2).
- Patchett P J, Kouvo O, Hedge C E, et al. Evolution of continental crust and mantle heterogeneity: Evidence from Hf isotopes[J]. *Contributions to Mineralogy and Petrology*, 1982, 78(3): 279-297.
- Petford N, Atherton M. Na-rich partial melts from newly underplated basaltic crust: the Cordillera Blanca Batholith, Peru[J]. *Journal of Petrology*, 1996, 37(6): 1491-1521.
- Porada H. Pan-African rifting and orogenesis in southern to equatorial Africa and eastern Brazil[J]. *Precambrian Research*, 1989, 44(2): 103-136.
- Porada H, Berhorst V. Towards a new understanding of the Neoproterozoic-Early Palaeozoic Lufilian and northern Zambezi Belts in Zambia and the Democratic Republic of Congo[J]. *Journal of African Earth Sciences*, 2000, 30(3): 727-771.
- Rainaud C, Master S, Armstrong R A, et al. Geochronology and

- nature of the Palaeoproterozoic basement in the Central African Copperbelt (Zambia and the Democratic Republic of Congo), with regional implications[J]. *Journal of African Earth Sciences*, 2005, 42(1–5): 1–31.
- Rapp R P, Watson E B. Dehydration melting of metabasalt at 8–32 kbar: implications for continental growth and crust-mantle recycling[J]. *Journal of Petrology*, 1995, 36(4): 891–931.
- Roberts M P, Clemens J D. Origin of high-potassium, talc-alkaline, I-type granitoids[J]. *Geology*, 1993, 21, 825–828.
- Roberts M P, Pin C, Clemens J D, et al. Petrogenesis of mafic to felsic plutonic rock associations: the Calc-alkaline Querigut Complex, French Pyrenees[J]. *Journal of Petrology*, 2000, 41, 809–844.
- Rolland Y, Galoyan G, Bosch D, et al. Jurassic back-arc and Cretaceous hot-spot series in the Armenian ophiolites: implications for the obduction process[J]. *Lithos*, 2009, 112: 163–187.
- Rudnick R L, Gao S. Composition of the continental crust[J]. In: Rudnick R L, Holland H D, Turekian K K, eds. *Treatise on Geochemistry*[M]. Elsevier-Pergamon, Oxford, 2003: 1–64.
- Scherer E, Munker C, Mezger K. Calibration of the lutetium-hafnium clock[J]. *Science*, 2001, 293: 683–687.
- Selley D, Broughton D, Scott R J, et al. A new look at the geology of the Zambian Copperbelt[J]. *Economic Geology*, 2005, 100: 965–1000.
- Shaw A, Downes H, Thirlwall M F. The quartz-diorites of Limousin: elemental and isotopic evidence for Devono-Carboniferous subduction in the Hercynian belt of the French Massif Central[J]. *Chemical Geology*, 1993, 107(1–2): 1–18.
- Smithies R H, Champion D C. The Archaean high-Mg diorite suite: links to tonalite-trondhjemite-granodiorite magmatism and implications for early Archaean crustal growth[J]. *Journal of Petrology*, 2000, 41: 1653–1671.
- Stein M, Hofmann A W. Mantle plumes and episodic crustal growth[J]. *Nature*, 1994, 372: 63–68.
- Stern R A, Hanson G N. Archean high-Mg granodiorite—a derivative of light rare-earth element-enriched monzodiorite of mantle origin. *Journal of Petrology*, 1991, 32, 201–238.
- Sun S S, McDonough W F. Chemical and isotopic systematics of oceanic basalts: implications for mantle composition and processes[J]. *Geological Society, London, Special Publications*, 1989, 42(1): 313–345.
- Tatsumi Y. Origin of high-magnesian andesites in the Setouchi volcanic belt, southwest Japan, II. Melting phase relations at high pressures[J]. *Earth and Planetary Science Letters*, 1982, 60(2): 305–317.
- Tembo F, Kampunzu A B, Porada H. Tholeitic magmatism associated with continental rifting in the Lufilian Fold Belt of Zambia[J]. *Journal of African Earth Sciences*, 1999, 28(2): 403–425.
- Unrug R. The Lufilian Arc: a microplate in the Pan-African collision zone of the Congo and the Kalahari cratons[J]. *Precambrian Research*, 1983, 21(3–4): 181–196.
- Vielzeuf D, Clemens J D, Pin C, et al. Granites, granulites, and crustal differentiation[J]. In: Vielzeuf D, Vidal P, eds. *Granulites and Crustal Evolution*[M]. Kluwer, Dordrecht, 1990: 59–85.
- Vinyu M L, Hanson R E, Martin M W, et al. U-Pb and $^{40}\text{Ar}/^{39}\text{Ar}$ geochronological constraints on the tectonic evolution of the easternmost part of the Zambezi orogenic belt, northeast Zimbabwe[J]. *Precambrian Research*, 1999, 98(1–2): 67–82.
- Wang Q, McDermott F, Xu J, et al. Cenozoic K-rich adakitic volcanic rocks in the Hohxil area, northern Tibet: lower-crustal melting in an intracontinental setting[J]. *Geology*, 2005, 33(6): 465–468.
- Wang Y J, Zhang A M, Fan W M, et al. Origin of paleosubduction-modified mantle for Silurian gabbro in the Cathaysia block: geochronological and geochemical evidence[J]. *Lithos*, 2013, 160: 37–54.
- Watters W A. Diorite and associated intrusive and metamorphic rocks between Port William and Paterson Inlet, Stewart Island, and on Ruapuke Island[J]. *New Zealand journal of geology and geophysics*, 1978, 21(4): 423–442.
- Wright J B. A simple alkalinity ratio and its application to questions of non-orogenic granite genesis[J]. *Geological Magazine*, 1969, 106(4): 370–384.
- Yuan H L, Gao S, Liu X M, et al. Accurate U-Pb age and trace element determination of zircon by laser ablation-inductively coupled plasma mass spectrometry[J]. *Geostandards and Geanalytical Research*, 2004, 28(3): 353–370.
- Zhao J H, Zhou M F, Zheng J P, et al. Neoproterozoic crustal growth and reworking of the Northwestern Yangtze Block: constraints from the Xixiang dioritic intrusion, South China[J]. *Lithos*, 2010, 120(3–4): 439–452.
- Zhou Y, Liang X, Liang X, et al. U-Pb geochronology and Hf-isotopes on detrital zircons of Lower Paleozoic strata from Hainan Island: new clues for the early crustal evolution of southeastern South China[J]. *Gondwana Research*, 2015, 27(4): 1586–1598.